Table 1. Bead movement and pollen tube growth rates (in micrometers per minute ± SD). Values represent mean rates of those beads and pollen tubes that traveled the farthest; n is number of gynoecia observed. Bead and pollen tube rates show no significant differences at $P < 0.02$, Mann-Whitney U test.

Species	Beads	Pollen tubes
H. flava	59.5 ± 17.6 (n = 7)	57.2 ± 23.9 (n = 5)
R. raphanistrum	20.7 ± 10.8 (n = 15)	16.1 ± 7.3 (n = 20)
V. faba	10.8 ± 3.2 (n = 6)	15.4 ± 4.8 (n = 12)

through the gynoecium to the ovules. Because there is no appreciable increase in cytoplasmic volume at the tip as the tube grows (*12*), the tip itself is essentially analogous to a moving cell, although older regions of the tube wall keep a connection to the pollen grain on the stigma surface. Cell movement in animals during embryogenesis occurs in an extracellular matrix composed of glycoproteins and proteoglycans (*13*). Researchers have demonstrated that nonliving particles can be transported along these matrices to distant locations (*14, 15*). The proposal in animal systems is that the cells themselves are not solely responsible for their movement but are facilitated by the matrix; hence, the phrase matrix-driven translocation. The secretory matrix of the gynoecium may actually interact with the pollen tube as it forms at the tip and may guide the tube toward the ovule. This could explain the directionality and rates of pollen tube growth seen in vivo, which are not seen in vitro. To date, research has focused mainly on a search for recognition molecules in self-incompatibility systems rather than on mechanisms for compatible tube growth. The molecules that have been isolated in self-incompatible systems are thought to interact somehow with the tube to stop growth; however, these molecules may also have a role associated with compatible pollen tube growth. Because self-compatibility is thought to be the ancestral condition in the angiosperms, additional research on the interactions of the pollen tube with the stigma and style in compatible crosses may provide insights into the mechanism of pollination and how it became modified in the evolution of self-incompatibility. The agent responsible for bead movement is not known, but these results describe a new kind of motility operating in plants.

REFERENCES AND NOTES

1. J. M. Picton and M. W. Steer, *J. Theor. Biol.* **98**, 15 (1982).
2. R. B. Knox, *Annu. Rev. Plant Physiol.* **17**, 508 (1984).
3. J. Heslop-Harrison, *Proc. R. Soc. London* **218**, 371 (1983).
4. A. E. Clarke, in *Extracellular Carbohydrates*, F. Loewus and W. Tanner, Eds. (Springer-Verlag, New York, 1981), pp. 517–582.
5. A. E. Clarke, P. Gleeson, S. Harrison, R. B. Knox, *Proc. Natl. Acad. Sci. U.S.A.* **76**, 3358 (1979).
6. Calculating diffusion rates: The following equation was used to determine the time needed for a 6-μm sphere to diffuse the longest distances beads had traveled in each species (*7*)

$$t = 3\pi\eta r x^2/kT$$

where k is Boltzmann's constant, 1.38×10^{-16} erg/K, and T is temperature in kelvins. These experiments occurred at room temperature, 300 K; η is the viscosity of the medium. We used the η for water to represent the secretions, that is, 1 cP or 0.01 g cm^{-1} s^{-1}. Sphere radius, r, was 3 μm, and x^2 (the distance squared) varied with each species. An example of how this equation was used is as follows: In *H. flava*, the longest observed distance the beads traveled was 31 mm; by the above equation, it would take 208 years for a 6-μm particle to diffuse that distance.
7. L. D. Landau and E. M. Lifshitz, *Fluid Mechanics* (Pergamon, London, 1959), p. 227.
8. J. P. Hill and E. M. Lord, *Am. J. Bot.* **74**, 988 (1987).
9. E. M. Lord and K. U. Kohorn, *ibid.* **73**, 70 (1986).
10. J. P. Mascarenhas, in *Receptors and Recognition*, G. L. Hazelbauer, Ed. (Chapman and Hall, London, 1978), pp. 171–203.
11. J. Heslop-Harrison, in *Biology of Reproduction and Cell Motility in Plants and Animals*, M. Cristi and R. Dallai, Eds. (Univ. of Siena Press, Siena, Italy, 1986), pp. 169–174.
12. K. R. Shivanna, B. M. Johri, D. C. Sastri, *Development and Physiology of Angiosperm Pollen* (Today and Tomorrow's Printers and Publishers, New Delhi, India, 1979), p. 59.
13. S. Dufour *et al.*, *Trends Genet.* **4**, 198 (1988).
14. M. Bronner-Fraser, *Dev. Biol.* **108**, 131 (1985).
15. S. A. Newman *et al.*, *Science* **228**, 885 (1985).

16. We thank P. Talbot and E. Nothnagel for discussion and advice. Supported by NSF grant PCM 851206202.

25 October 1988; accepted 27 December 1988

Commitment of Neural Crest Cells to the Sensory Neuron Lineage

MAYA SIEBER-BLUM

Clonal cultures and monoclonal antibodies against a lineage-specific epitope, stage-specific embryonic antigen-1 (SSEA-1) were used to analyze the commitment of quail neural crest cells to the sensory neuron pathway. There were two distinct populations of sensory cells at the time of gangliogenesis. Postmitotic neuroblasts that remained in close association with the neural tube coexisted with a large number of pluripotent cells that formed the leading edge of the emigrating cells and gave rise to sensory and autonomic neuroblasts and to melanocytes. The data suggest a dual origin of spinal sensory neuroblasts and a predominantly late divergence of the autonomic and sensory lineages.

AUTONOMIC NEURONS, AS WELL AS spinal and some cranial primary sensory neurons, are derived from the neural crest (*1–3*). However, the mechanisms that regulate the formation of the autonomic and sensory nervous systems are poorly understood. We used clonal cultures and antibodies against SSEA-1 to probe the spinal sensory neuron lineage in the quail neural crest. We found a temporally and spatially dual origin of spinal sensory neuroblasts. The data indicate that the predominant mechanism is segregation of the adrenergic and sensory lineages after formation of the sensory ganglia is initiated. In addition, however, there are a number of early-differ-

Department of Anatomy and Cellular Biology, Medical College of Wisconsin, Milwaukee, WI 53226.

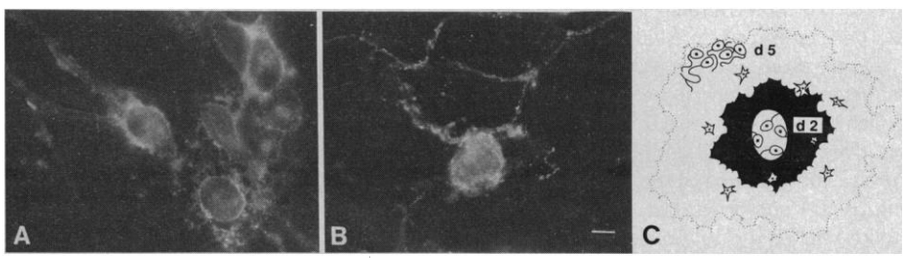

Fig. 1. Two subpopulations of SSEA-1–immunoreactive (*27*) cells in primary neural crest cell cultures. (**A**) Centrally located SSEA-1^+ sensory neuroblasts on day 14 that were attached to a neural tube remnant. (**B**) Peripherally located SSEA-1–immunoreactive cell on day 21. (**C**) Schematic drawing of a primary neural crest cell culture. Centrally located sensory neuroblasts appeared on day 2 (E4) and were surrounded by a ring of pigment cells (darkly shaded area), which were located on top of unpigmented cells and appeared on days 3 to 4. Multipolar adrenergic neuroblasts (TH^+ and DBH^+) first appeared on days 3 to 4 at both sides of the margin of the area containing pigmented cells. A second population of SSEA-1^+ cells appeared in peripheral areas. Occasional SSEA-1^+ cells were observed as early as on culture day 5 (E7), large numbers by day 8.

entiating sensory neuroblasts that remain in close association with the neural tube.

SSEA-1 (*4*) belongs to the lactoseries type 2 carbohydrate antigens that are characterized by a Galβ1→4GlcNAc backbone sequence. In the rat it is present in a subset of postmitotic primary sensory neurons. This and other carbohydrate antigens may play a role in the specific innervation of the dorsal horn (*5–7*). We established that SSEA-1 is a specific marker for primary sensory neurons in quail embryos. SSEA-1 was expressed by all detectable sensory neurons at all spinal axial levels of the trunk. By contrast, adrenergic neuroblasts were not stained by antibodies to SSEA-1. They were, however, immunoreactive to tyrosine hydroxylase (TH) (*8*). Sensory neuroblasts are thus defined as SSEA-1^+/TH^-, and adrenergic neuroblasts as SSEA-1^-/TH^+ cells.

In primary neural crest cell cultures (*9*) there were two discrete populations of SSEA-1^+ cells. One population first appeared on day 2 of culture [corresponding to embryonic day 4 (E4)] on top of a centrally located dorsal neural tube remnant (Fig. 1, A and C). These cells failed to emigrate from the neural tube and constituted only 0.02 to 0.1% of all neural crest cells in the culture (two to ten SSEA-1^+ cells per ~10^4 neural crest cells on day 2). The same cells reacted with the monoclonal antibody HNK-1 and antibodies against substance P and glutamate, identifying them as neural crest–derived sensory neuroblasts (*8, 10, 11*). Contrary to expectations, a second population of SSEA-1–immunoreactive cells emerged at the periphery of the culture by day 5 (E7) (Fig. 1, B and C). Their progenitors, the early emigrating crest cells, were cloned by limiting dilution (*12*) on culture day 1 (E3), that is, at the time spinal ganglion formation is initiated in the embryo (*13*).

There were three classes of clone-forming progenitor cells that could be distinguished by the differentiated progeny they generated (unpigmented, mixed, and pigmented clones) (*12*) and their affinity for a lipophilic plasma membrane probe, merocyanine 540 (*14*). Approximately one-third of the cloned cells were virtually nonproliferative and remained stellate or fibroblastic. Some of them may have been cells that had been damaged during trypsinization; others may have been unidentifiable phenotypes of neural crest or non–neural crest origin. These cells were not analyzed further. Another one-third of the cells were committed to the melanogenic lineage, that is, they gave rise to fully pigmented clones. The remaining one-third generated unpigmented and mixed clones. Figure 2 shows a typical example of the development of a mixed clone.

By day 4, approximately 30 pigmented cells appeared almost simultaneously in different locations of the clone. By day 5, proliferation of pigmented cells slowed, whereas unpigmented cells continued to divide at a high rate with a generation time of about 12 hours (*15*). After 2 to 3 weeks, unpigmented and mixed clones consisted of several thou-

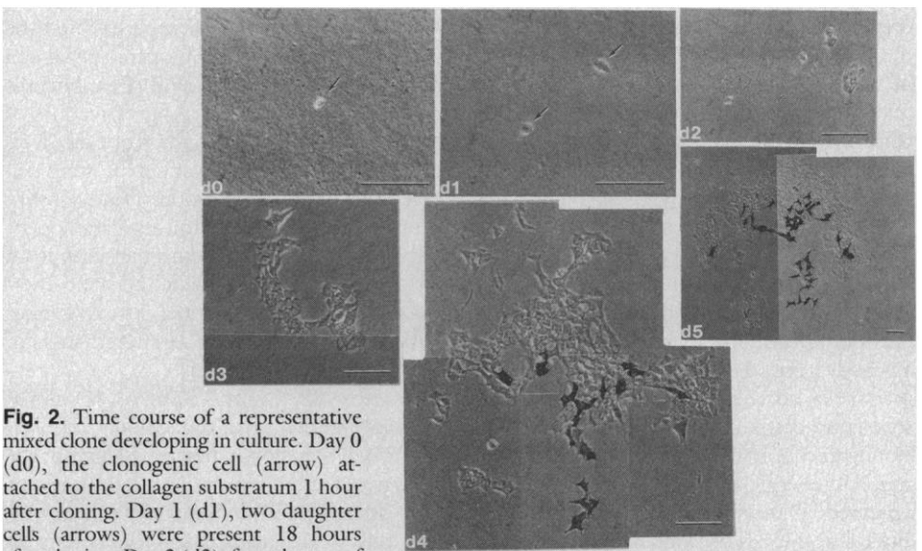

Fig. 2. Time course of a representative mixed clone developing in culture. Day 0 (d0), the clonogenic cell (arrow) attached to the collagen substratum 1 hour after cloning. Day 1 (d1), two daughter cells (arrows) were present 18 hours after cloning. Day 2 (d2), four clusters of highly motile cells. Day 3 (d3). Day 4 (d4), approximately 30 pigment cells appeared over a 4- to 8-hour period. Day 5 (d5), the number of pigmented cells increased by slowed proliferation of already pigmented melanocytes; unpigmented cells divided at a high rate. Bars, 100 μm.

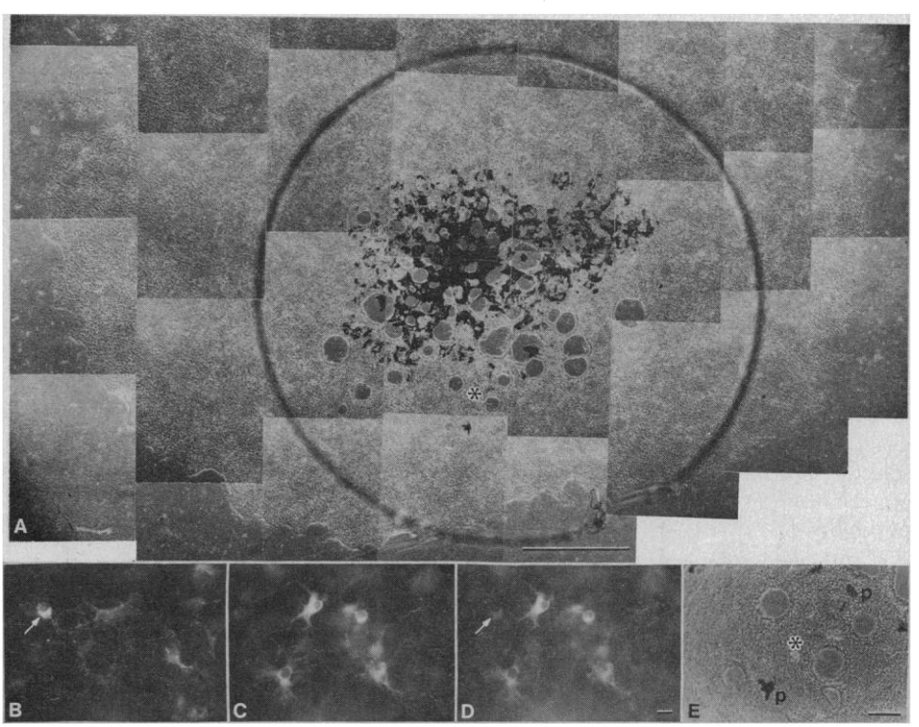

Fig. 3. Double labeling (*27*) with antibodies against SSEA-1 and TH in a mixed clone 22 days after cloning. (**A**) Phase-contrast photomicrograph of part of a mixed clone. The circular mark was made on the underside of the culture dish at the time of cloning to indicate the position of the drop of culture medium containing the clonogenic cell. Asterisk, position of field in (B) to (D). Bar, 1 mm. (B to E) Selected field showing SSEA-1^+/TH^- cells, SSEA-1^-/TH^+ cells, and pigment cells. (**B**) Rhodamine fluorescence of SSEA-1–immunoreactive cells. Arrow, sensory neuroblasts with rounded soma and one process. (**C**) Fluorescein fluorescence of TH-immunoreactive cells in the same field. (**D**) Double exposure. Arrow, same cell marked in (B). Bar, 10 μm. (**E**) Larger area of same field with phase-contrast optics at lower magnification showing scattered pigment cells (p). Bar, 100 μm. Asterisk, position of field in (B) to (D).

sand cells and reached diameters of several millimeters (Fig. 3).

On day 22, clones were analyzed for the presence of autonomic and sensory neurons. We used monoclonal antibodies to SSEA-1 as well as polyclonal antibodies to TH and dopamine-β-hydroxylase (DBH) to analyze three unpigmented and three mixed clones in addition to ten unpigmented and ten mixed colonies grown in sparse secondary cultures. All 26 clones and colonies contained both SSEA-1^+/TH^- (or SSEA-1^+/DBH^-) sensory and SSEA-1^-/TH^+ (or SSEA-1^-/DBH^+) adrenergic neuroblasts. The unpigmented and mixed clones both contained several hundred sensory and adrenergic neuroblasts and hundreds of cells that did not bind detectable levels of either antibody (Fig. 3). The coexistence of pigment cells, adrenergic neuroblasts, and sensory neuroblasts in a clone implies that the clonogenic cell was at least tripotent. Because adrenergic and sensory cells were also observed in unpigmented clones, we conclude that there is a second class of precursor cells that are at least dipotent and have lost the ability to generate pigment cells.

The dichotomous origin of spinal sensory neuroblasts resolves several apparently conflicting earlier reports. Le Douarin and colleagues (*16*) proposed an early segregation of the adrenergic and sensory lineages, whereas clonal analyses (*17, 18*) suggested the existence of a common progenitor cell in the neural crest after migration. Our data indicate that both mechanisms occur simultaneously. The early-differentiating sensory neuroblasts may be identical with the postmitotic neuroblasts observed in culture by Ziller *et al.* (*19*), and their function may be similar to that of Rohon-Beard cells in amphibians. Alternatively, early postmitotic cells may give rise to ventrolateral neuroblasts, and pluripotent cells may generate dorsomedial neuroblasts in dorsal root ganglia (*20*). However, the presence of substance P–like immunoreactive cells in both populations (*8*) argues against the latter possibility.

The dual origin of sensory neuroblasts also occurs in other systems. For instance, rat astrocytes arise from two separate lineages. Type I astrocytes differentiate before birth, whereas type II astrocytes develop after birth from a bipotent glial progenitor cell that also generates oligodendrocytes (*21*). Furthermore, as shown here, some melanogenic cells are determined by culture day 1 (E3) and give rise to fully pigmented clones; others are determined by about E5 and are part of mixed clones.

The presence of cells in dorsal root ganglia that retain the capacity to generate melanocytes (Fig. 4) agrees with earlier observations of pigmentation in explanted embryonic dorsal root ganglia by Nichols *et al.* (*22*). Because neural crest cells in clonal culture divide with a generation time of 12 hours (*15*), the almost simultaneous appearance of about 30 pigmented cells on day 4 in mixed clones puts the earliest possible time of segregation of the melanogenic lineage in mixed clones at culture day 2 (E5). Nichols *et al.* (*22*) also noticed a progressive loss of melanogenesis when ganglia from day 5 or older embryos were explanted. A stem cell that is common to autonomic and sensory neuroblasts and persists during gangliogenesis also explains the finding that cells from early spinal ganglia populate the sympathetic ganglia when transplanted into a younger host embryo and express adrenergic traits in vivo and in vitro (*16, 23*).

In vitro (*12, 24*) and in vivo (*18*) clonal analyses and the use of monoclonal antibodies (*25*) have shown heterogeneity in the early neural crest, contradicting the concept of a homogeneous population of pluripotent cells (*1*). The five subpopulations of cells observed in this study (SAP, SA, S, P, and nonproliferating; Fig. 4) suggest that the early neural crest contains both pluripotent cells and cells with a restricted developmental potential. The exact timing and the mechanism of the segregation of the adrenergic and sensory lineages from pluripotent progenitor cells remain to be established. Brain-derived neurotrophic factor promotes survival of early postmitotic sensory neuroblasts (*26*). This factor or a similar central nervous system–derived factor may play a role in the commitment of neural crest cells to the sensory neuron lineage.

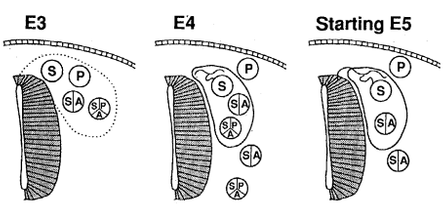

Fig. 4. A model of the time course of commitment of quail neural crest cells to the spinal sensory neuron, adrenergic neuron, and melanocyte phenotypes. The neural crest gives rise to sensory (S), autonomic (A), and pigment cells (P). On embryonic day 3 (E3) at the time of ganglion formation (*15*), the migrating population is composed of cells that are at least tripotent (S, A, and P), at least bipotent (S and A), and committed to the melanogenic (P) and possibly other, here unidentified, lineages. A hypothetical cell committed to the sensory lineage (S) remains in close association with the neural tube. By E4, S cells start to become postmitotic and elaborate neurites. In addition, SAP tripotent and SA dipotent cells populate the dorsal root ganglia (that is, cells within solid line) and possibly the sympathetic ganglia. Presumptive melanocytes migrate along the dorsolateral pathway below the ectoderm. These may be the committed cells (P) that form fully pigmented colonies in clonal culture. Starting at E5, the SAP tripotent cells begin to disappear. The sensory and adrenergic lineages segregate last.

REFERENCES AND NOTES

1. J. A. Weston, *Adv. Morphog.* **8**, 41 (1970).
2. D. Noden, in *Specificity of Embryological Interactions, Receptors and Recognition,* D. R. Garrod, Ed. (Chapman and Hall, London, 1978), pp. 3–49.
3. N. Le Douarin, *The Neural Crest* (Cambridge Univ. Press, Cambridge, 1982).
4. D. Solter and B. B. Knowles, *Proc. Natl. Acad. Sci. U.S.A.* **75**, 5565 (1978).
5. J. Dodd and T. M. Jessell, *J. Neurosci.* **5**, 3278 (1985).
6. T. M. Jessell and J. Dodd, in *Neuropeptides in Neurologic and Psychiatric Disease,* J. B. Martin and J. D. Barchas, Eds. (Raven, New York, 1986), pp. 111–133; L. J. Regan *et al.*, *Proc. Natl. Acad. Sci. U.S.A.* **83**, 2248 (1986).
7. J. Dodd *et al.*, *Nature* **311**, 469 (1984).
8. M. Sieber-Blum, in preparation.
9. A. M. Cohen and I. R. Konigsberg, *Dev. Biol.* **46**, 262 (1975). The last six segments (somite levels 16 to 22) of stage 14 embryos (at 48 hours of incubation) were dissected and treated with dispase (grade II, 25 U/ml; Boehringer) to dissociate the tissue.
10. M. Sieber-Blum, S. R. Kumar, D. R. Riley, *Dev. Brain Res.* **39**, 69 (1988).
11. J. Ritland and M. Sieber-Blum, in preparation.
12. M. Sieber-Blum and A. M. Cohen, *Dev. Biol.* **80**, 96 (1980); M. Sieber-Blum and F. Sieber, in *Cell Culture in the Neurosciences,* J. E. Bottenstein and G. Sato, Eds. (Plenum, New York, 1985), pp. 193–222. Neural crest cells from 24-hour primary cultures (corresponding to E3) were cloned. The neural tubes were completely removed to separate peripheral from central sensory progenitors. In a typical experiment, out of a total of 100 plates filled, 18 contained single cells. Of these, two died during the first 24 hours, and six had a "low proliferation potential" (0 to 1 cell division during the first 2 days in culture) and were thus excluded from the study. Of the remaining ten clones, five became pigmented, three mixed, and two unpigmented. The adrenergic phenotype was first observed at day 11 (*12*); the clones were analyzed at day 22.
13. T. E. Lallier and M. Bronner-Fraser, *Dev. Biol.* **127**, 99 (1988).
14. M. Sieber-Blum and F. Sieber, *Dev. Brain Res.* **14**, 241 (1984).
15. ———, *Differentiation* **20**, 117 (1981).
16. C. Le Lievre *et al.*, *Dev. Biol.* **77**, 362 (1980); N. M. Le Douarin, in *Cellular and Molecular Biology of Neuronal Development,* I. B. Black, Ed. (Plenum, New York, 1984), pp. 3–26; N. M. Le Douarin, *Science* **231**, 1515 (1986).
17. M. Sieber-Blum, *Soc. Neurosci. Abstr.* **14**, 319 (1988).
18. M. Bronner-Fraser and S. E. Fraser, *Nature* **335**, 161 (1988).
19. C. Ziller *et al.*, *Cell* **32**, 627 (1983).
20. V. M. Carr and S. B. Simpson, *J. Comp. Neurol.* **182**, 727 (1978).
21. M. C. Raff, E. R. Abney, R. H. Miller, *Dev. Biol.* **106**, 53 (1984).
22. D. H. Nichols *et al.*, *ibid.* **60**, 226 (1977).
23. Z. G. Xue, J. Smith, N. M. Le Douarin, *Proc. Natl. Acad. Sci. U.S.A.* **82**, 8800 (1985).
24. A. Baroffio, E. Dupin, N. M. Le Douarin, *ibid.* **85**, 5325 (1988).
25. K. F. Barald, in *Neuronal Development,* N. C. Spitzer, Ed. (Plenum, New York, 1982), pp. 101–119; J. Girdlestone and J. A. Weston, *Dev. Biol.* **109**, 274 (1985); M. F. Marusich, K. Pourmehr, J. A. Weston, *ibid.* **118**, 494 (1986); M. Barbu, C. Ziller, P. M. Rong, N. M. Le Douarin, *J. Neurosci.* 6, 2215 (1986).
26. U. Ernsberger and H. Rohrer, *Dev. Biol.* **126**, 420 (1988).
27. For indirect immunofluorescence, the protocol was the same as in (*10*). In double-staining experiments, both primary antibodies (in the presence of 0.1% Triton X-100 in phosphate-buffered saline) were

combined and used at the following final concentrations: AC4 hybridoma culture supernatant (monoclonal antibody recognizing SSEA-1), 1:1; antibody to SSEA-1, 1:200; polyclonal rabbit antibodies against TH and DBH (Eugene Tech International, Inc., Allendale, NJ), 1:60. Secondary antibodies (fluorescein- and rhodamine-conjugated affinity-purified goat antibodies to rabbit immunoglobulins and goat antibodies to mouse gamma globulins; Organon Teknika, Malvern, PA) were added together as well at a final concentration of 1:10.

28. I thank D. Noden for stimulating discussions; J. Dodd, T. Jessell, and D. Solter for gifts of AC4 and antibody to SSEA-1; J. Wright for technical assistance; C. Snyder and S. Tjepkema-Burrows for help with the illustrations; and D. Riley, F. Sieber, and M. Wong-Riley for critically reading the manuscript. Supported by USPHS grant HD21423 from the National Institute of Child Health and Human Development.

31 October 1988; accepted 31 December 1988

Indole-2-Carboxylic Acid: A Competitive Antagonist of Potentiation by Glycine at the NMDA Receptor

JAMES E. HUETTNER

The *N*-methyl-D-aspartate (NMDA) class of excitatory amino acid receptors regulates the strength and stability of excitatory synapses and appears to play a major role in excitotoxic neuronal death associated with stroke and epilepsy. The conductance increase gated by NMDA is potentiated by the amino acid glycine, which acts at an allosteric site tightly coupled to the NMDA receptor. Indole-2-carboxylic acid (I2CA) specifically and competitively inhibits the potentiation by glycine of NMDA-gated current. In solutions containing low levels of glycine, I2CA completely blocks the response to NMDA, suggesting that NMDA alone is not sufficient for channel activation. I2CA will be useful for defining the interaction of glycine with NMDA receptors and for determining the in vivo role of glycine in excitotoxicity and synapse stabilization.

VERTEBRATE CENTRAL NEURONS express two classes of excitatory amino acid receptors that mediate synaptic transmission throughout the brain and spinal cord (*1*). Fast transmission of single impulses involves mainly the kainate-quisqualate receptor class. A number of integrative phenomena, including long-term potentiation and eye-specific terminal segregation, require activation of the second receptor type (*2*), which is named for the selective agonist NMDA (*1*). Binding of transmitter to NMDA receptors activates ion channels that conduct monovalent cations and Ca^{2+} (*3*). Several additional factors regulate the conductance increase elicited by NMDA: (i) extracellular Mg^{2+} produces voltage-dependent block of the ion channel (*4*); (ii) Zn^{2+} inhibits channel opening by a different mechanism that is much less voltage-dependent (*5*); and (iii) the amino acid glycine (*6*) greatly increases the frequency of channel openings evoked by NMDA but does not open the channel when applied alone. The high affinity of the glycine potentiation site [half-maximal dose (EC_{50}) = 100 to 700 n*M*] has made it difficult to assess the role of glycine in vivo, because extracellular fluid is likely to contain a saturating concentration of glycine. Recent work (*7, 8*) on NMDA receptors expressed in *Xenopus* oocytes has raised the possibility that glycine may be absolutely required for NMDA-gated channels to open; the small current observed in the absence of added glycine could be due to nanomolar levels of contaminating glycine typically found in physiological solutions (*6, 7*). Interest in these problems has sparked a search for antagonists of the glycine potentiation site (*9*). I report that I2CA (Fig. 1) and several active derivatives competitively inhibit the action of glycine on the NMDA receptor.

Current elicited by NMDA was recorded in primary cultures of the rat visual cortex or spinal cord (*10*) with the whole-cell configuration of the patch-clamp technique (*11, 12*). In agreement with earlier work (*6–8*), glycine produced a dose-dependent increase in whole-cell current evoked by NMDA (Fig. 2). At −70 mV, NMDA activated only a few picoamperes of current in the absence of added glycine (see below); saturating concentrations of glycine potentiated the response to NMDA by 5 to 100 times. The dose-response relation for glycine can be fitted well by the equation for one-to-one binding (Fig. 2C) (*7, 8*), which suggests that the physiological response to glycine is directly proportional to receptor occupancy. I2CA and several active derivatives competitively antagonized the potentiation by glycine, causing a shift in the dose-response relation to higher glycine concentrations

Department of Neurobiology, Harvard Medical School, 220 Longwood Avenue, Boston, MA 02115.

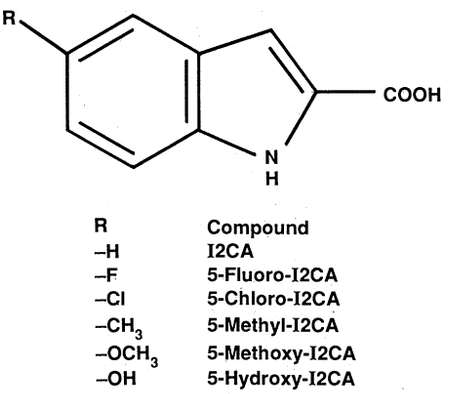

R	Compound
–H	I2CA
–F	5-Fluoro-I2CA
–Cl	5-Chloro-I2CA
$–CH_3$	5-Methyl-I2CA
$–OCH_3$	5-Methoxy-I2CA
–OH	5-Hydroxy-I2CA

Fig. 1. Chemical structures of I2CA and five substituted derivatives of I2CA.

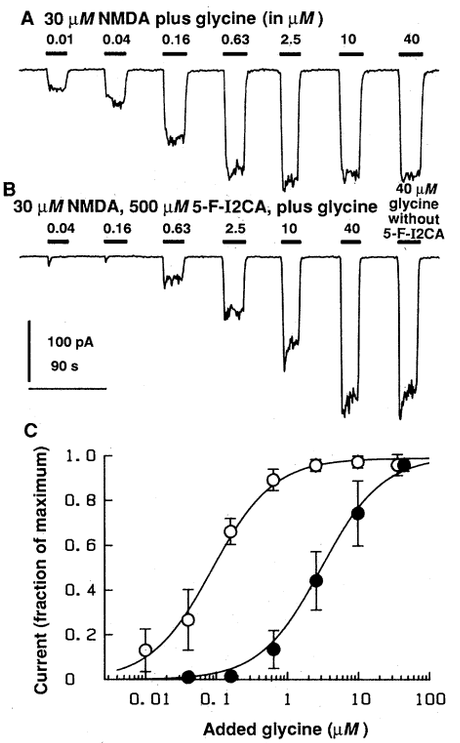

Fig. 2. The potentiation by glycine of current gated by NMDA is inhibited by 5-F-I2CA. (**A**) Whole-cell recording of current activated by 30 μ*M* NMDA plus 10 n*M* to 40 μ*M* added glycine; holding potential, −70 mV. (**B**) In the same cell, current activated by 30 μ*M* NMDA plus 40 n*M* to 40 μ*M* glycine in the presence of 500 μ*M* 5-F-I2CA and by 30 μ*M* NMDA plus 40 μ*M* glycine without 5-F-I2CA. Cortical neuron 8G19A from a P 5 donor, 6 days in vitro. (**C**) Dose-response relation for glycine in three neurons in the absence (○) or presence (●) of 500 μ*M* 5-F-I2CA; 30 μ*M* NMDA was included in each test solution. Points show mean ± SD of the current averaged over the last 10 to 20 s of each application, plotted as a fraction of the maximal current. The full dose-response relation for glycine alone and for glycine plus 5-F-I2CA was measured in three cortical neurons a total of eight times. The curves are least-squares fits of the Langmuir equation (*13*), with EC_{50} = 89 n*M* (○) or 3 μ*M* (●). The dose-response relation for glycine was also shifted to the right by I2CA, 5-Cl-I2CA, 5-methyl-I2CA, and 5-methoxy-I2CA.